MINISTRY OF EDUCATION AND TRAINING

VIETNAM ACADEMY OF SCIENCE AND TECHNOLOGY

GRADUATE UNIVERSITY OF SCIENCE AND TECHNOLOGY

TRẦN VĂN PHÚC

STUDY ON APPLICATION OF THE NUCLEAR METHODS FOR ANALYSIS TIO_2/SIO_2 MATERIAL USING ACCELERATED ION BEAM

Major: Atomic Physics
Code: 9440106

SUMMARY OF ATOMIC PHYSICS DOCTORAL THESIS

Hanoi – 2023

Công trình được hoàn thành tại: Học viện Khoa học và Công nghệ - Viện Hàn lâm Khoa học và Công nghệ Việt Nam.

Người hướng dẫn khoa học 1: GS.TS. Lê Hồng Khiêm – Viện Vật Lý, VHLKH&CNVN
Người hướng dẫn khoa học 2: TS. Miroslaw Kulik – Viện Liên Hiệp Nghiên Cứu Hạt Nhân (JINR), Dubna, Liên Bang Nga

Phản biện 1: …
Phản biện 2: …
Phản biện 3: ….

Luận án sẽ được bảo vệ trước Hội đồng đánh giá luận án tiến sĩ cấp Học viện, họp tại Học viện Khoa học và Công nghệ - Viện Hàn lâm Khoa học và Công nghệ Việt Nam vào hồi … giờ … ngày … tháng … năm 201….

Có thể tìm hiểu luận án tại:
- Thư viện Học viện Khoa học và Công nghệ
- Thư viện Quốc gia Việt Nam

PREAMBLE

1. The urgency of the thesis

For the application of ion beams to modify material structures, ion implantation is the most typical method. It is a well-known fact that the structures and properties of materials can be modified in a controlled way by means of the ion implantation technique [1]. For multilayer materials, once a target is bombarded with an appropriate ion beam, ion beam mixing (IBM) occurs in the regions between material layers, even in the normal experimental conditions [2]. IBM has thus become an effective approach to customizing the properties of multilayer materials, especially when the traditional methods, e.g., deposition or thermal processing, do not succeed. In fact, creating stable, metastable, amorphous, and crystalline phases in bilayer and multilayer materials has been common use of the IBM [3,4]. Many material systems involving metal-metal [5,6], metal-silicon [7,8] or metal-insulator systems have been employed for studies on IBM's fundamental mechanisms and prospective applications [9]. However, the fundamental mechanism of the IBM and how it affects the properties of irradiated materials have not been fully understood. One has known that there exists an optimum combination of thickness of the over-layer thin film and the ion beam parameters to enhance the interfacial mixing yield, whereas the dependence of mixing amount on ion fluence and deposited energy can be predicted using mixing models [10,11]. Nevertheless, the precise recipe for finding that optimum combination and understanding the modification of the parameters of the mixing models are still under development. The main difficulty comes from the fact that the mixing is not merely a simple function of ion energy and mass.

Furthermore, unlike metal/metal, metal/silicon, and metal/insulator systems, where the mixing mechanism is rather understood, data on oxide/oxide systems is sparse. In the energy range of 100 – 250 keV, there was no report on the influence of ion energy and mass on atomic mixing also the changes in properties of oxide/oxide materials. Therefore, the mechanism and potential of ion mixing for modifying the interfacial properties of oxide/oxide systems have yet to be adequately determined. Relatively few systems have been studied, and the range of experimental conditions has been limited. In principle, because most oxide-oxide reactions are neither extremely exothermic nor highly endothermic, it is difficult to anticipate how much ion-induced interfacial mixing will occur. Additionally, it is unclear whether ion mixing promotes the formation of glassy oxide mixtures or separates the oxide phases. These factors greatly influence the adhesion enhancement expected from ion mixing.

Therefore, the mechanism of mixing induced by irradiation associated with changes in oxide material properties is essential to be investigated. This work is directed toward obtaining a better understanding of mixing characterization and the relative roles of kinetics in oxide-oxide bilayer mixing.

Among the double antireflective self-cleaning coatings for photovoltaic solar cells, such as Al_2O_3/SiO_2, TiO_2/SiO_2, Si_3N_4/MgF_2, the most widely used system is TiO_2/SiO_2 due to their excellent adhesion and transmittance [12,13]. On the one hand, due to the tunable refractive index, SiO_2 was considered to achieve high antireflection property [14]. On the other hand, two photo-induced phenomena: photo-induced hydrophilicity and photocatalysis of TiO_2 film made it self-cleaning [15]. It has been proved that TiO_2 and SiO_2 coatings on solar cells reduced the reflection of solar cells from 36% to 15% with a single-layer (SiO_2) and to 7% with a double-layer (TiO_2/SiO_2) [16]. When used normally, TiO_2/SiO_2 needs to be resistant to environmental aggression that might arise. The key to achieving excellent antireflection performance is the control of coatings' refractive index (n). This means that absorption in materials and at interfaces should be kept to a minimum and the refractive index should remain constant over time [17]. Accordingly, it is important to know how the interface is formed and their thickness results in a variation of the index and possibly absorption. It has been proved that the thickness of interface area between materials is well controlled by IBM [7]. Nevertheless, the implantation necessary to mix an oxide/oxide interface might cause significant damage, which is undesirable for the majority of thin-film applications [18]. Therefore, to understand the overall irradiation response of the TiO_2/SiO_2 bilayer, further studies on irradiation-induced defects and the corresponding changes in interfacial properties are essential.

2. The purpose and tasks of the research

The first goal of the thesis is to grasp the principles, experiments and applications of the Rutherford Backscattering Spectrometry (RBS) method in the analysis of materials, especially multilayer materials. Approach to the scientific problems as well as modern research directions in the world toward the research on application of ion beam in modification and analysis of materials.

The thesis focuses on describing and analyzing the atomic mixing phenomenon that occurs at the material interface after ion implantation using the RBS method. Investigate the variation in the degree of atomic mixing through experimental parameters that cannot be predicted by theoretical models, and explain the phenomena by Monte Carlo simulation. In addition,

analyze the chemical and optical properties of the samples after being implanted with noble gas ions by Xray Photoelectron Spectroscopy (XPS) and Ellipsometry Spectroscopy (ES) methods.

3. The object and scope of the research

i) Characterization changes in structure of the $TiO_2/SiO_2/Si$ systems, including the transition layers between TiO_2 and SiO_2 induced by noble gases ion irradiation in the energy range of 100-250 keV using one of the ion beam analysis methods - Rutherford Backscattering Spectrometry (RBS).

ii) Investigation dependence of ion-induced mixing at TiO_2/SiO_2 interface on the energy and mass of incident ions with different thickness of material layers.

iii) Interpretation of mixing mechanism in term of kinetic atomic transport using Stopping and Range of Ions in Matter (SRIM) simulation.

iv) Study on influence of changes in chemical composition induced by ion irradiation on mixing amount as function of ion energy using XPS method.

v) Investigation changes in optical parameters of un-irradiated and irradiated TiO_2/SiO_2 transition area as function of ion energy using the ES method.

CHAPTER I
INTRODUCTION

1.1. Low-energy ion modification of solids and ion beam mixing process

During low energy ion irradiation, particularly with heavy ions, the structure and composition of the surface layers of a sample can be substantially modified. There are four main processes (Fig.1.1) involved: ion implantation - the introduction of a new atomic species; radiation damage - the displacement of sample atoms; ion beam mixing - the promotion of diffusion and migration of atomic species; and sputtering - the ejection of surface atoms.

The near-surface composition of a sample can be substantially modified by ion implantation (Fig.1.1a) and this is now widely used for changing materials properties. When ions lose energy in nuclear collisions with target atoms, many atoms are displaced from their normal locations. Target atoms recoiling from these collisions can themselves carry enough energy to cause additional displacements sometimes producing a collision cascade which affects many atoms at a distance from the original ion path (Fig.1.1b). Ion irradiation can also promote diffusion through both collisional effects and increases in local temperature in the irradiated region (Fig.1.1c). Ion beam mixing of atomic constituents is a process which can be usefully exploited for the development of new materials but it can also change the target composition during ion beam analysis, particularly when high fluences of heavy ions are employed. The unique features of ion beam mixing are the spatial selectivity and no requirement for heat treatment. The sputtering accompanies collision cascades which cause target atoms to be ejected (Fig. 1.1d). Sputtering is an important method for the controlled removal of surface layers from a solid.

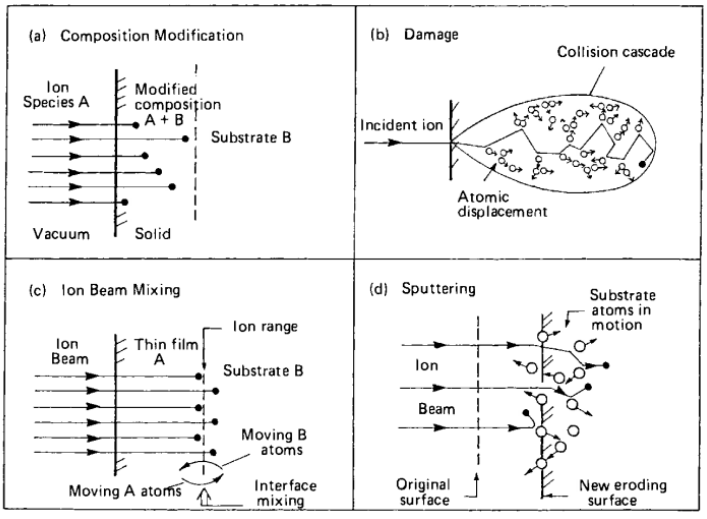

Fig.1.1. Schematic illustration of four ion beam modification processes [19].

1.2. Concept of ion beam mixing

Ion beam mixing is the process of atoms from several atomic species merging across an interface under the influence of an ion beam. When energetic ions interact with nuclei and electrons of a solid, their energy is deposited in the substance. The formation of a moving atoms cascade is one of the effects of energy transfer to target atoms. If the ion energy is high enough to penetrate beyond the interface between two materials A and B, the recoiling atoms created near the interface may have sufficient energy to cross it. Intermixing of A and B atoms in the interface region therefore is the outcome.

There are three types of the sample configurations that are used commonly in the ion beam mixing study. The first type, a thin maker of element A is placed between two layers of material B. The system approximates the spreading of impurity A in a matrix made up largely of B atoms with the typical thickness of layer A is about 1 nm. The second type of geometry, thin film of element A is evaporated onto substrate B. During ion bombardment, A and B form a semi-infinite diffusion couple and are free to form continuous solid solutions, intermediate phases or compounds. The third type of sample design, is made up of alternate thin evaporated layers (multilayers) of A and B with an overall thickness less than the ion range. To be merged with the opposite layer, A (or B) atoms now must be displaced only a few interatomic lengths. In this thesis, the configuration of the bilayer has been utilized for the ion beam mixing studies.

The basic process involved in low energy ion beam mixing is illustrated schematically in Fig.1.2. When the energetic heavy ion penetrates a top (impurity) layer A to reach a bulk material B, it loses energy due to collision with target atoms, which receive sufficient energy to get displaced from their original positions. These displaced atoms in turn make multiple collisions with the target atoms to produce a displacement cascade. The displacement of atoms occurring near the interface of layer A and the bulk material B results into a mixed region of A and B. The compositional changes achieved by ion beam mixing of an A–B interface, where A and B denote different materials turned out to be much faster as compared to implantation of A into B.

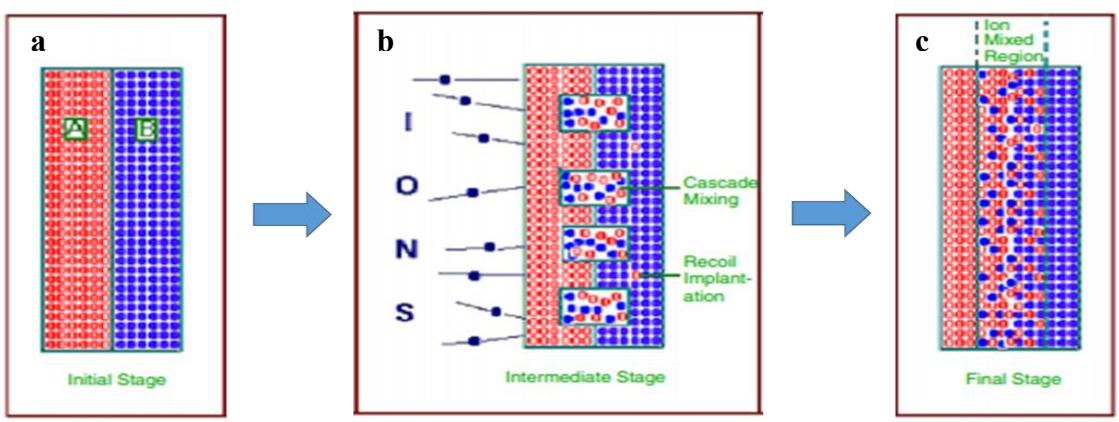

Fig.1.2. The formation process of transition layer during ion irradiation [20].

The effects of these collisions can be divided into two mechanisms based on the time scales: prompt effects (~ a few ps) termed as *ballistic mixing* including *recoil implantation* and *cascade mixing*; delayed effects (exceeding several ns) termed as *thermal mixing* consisting of *Radiation Enhanced Diffusion* (RED) at higher temperatures and *thermal spike* diffusion at lower temperatures. In the present work, the contribution of the recoil and cascade to ion mixing will be investigated, mechanism of this process is given in the following sections.

In literature, it indicates that the dependence of mixing degree on ion fluence ∅ and energy deposited per unit depth F_D has been well established by both experimental studies using the primary RBS method and model-based calculations. However, choosing a convenient mixing model depends on ion beam parameters and the target properties (or material configuration). Mixing degree do not depend directly on the factors as samples temperature, ion charge state, ion energy, or ion mass. Effects of these parameters on mixing of different material configurations has been carried out experimentally. Moreover, most investigations of ion-induced mixing have dealt with metal films on oxide, polymer, semiconductor, and metal substrates. The mixing behavior and potential of ion mixing for modifying the interfacial properties of oxide/oxide systems have yet to be adequately determined.

CHAPTER 2
THE EXPERIMENTAL TECHNIQUES

In order to investigate the mixing and changes in interfacial properties of the TiO_2/SiO_2 systems induced by ion implantation, the Rutherford Backscattering Spectrometry (RBS), Ellipsometry Spectroscopy (ES), and X-ray Photoelectron Spectroscopy (XPS) methods has been used. The techniques can be classified into major – ion implantation and RBS, and auxiliary – XPS and ES. In this chapter, a short discussion of physical concepts of the techniques will be given, followed by the experimental conditions.

2.1. Ion implantation

Ion implantation has proved its superiority over diffusion in integrated circuit technology because of the precise control which it offers over the doping level and the thickness of the doped layer. In addition, it has good reproducibility and can be used for doping selected areas by masking procedures. The collisional nature of ion implantation makes it a violent technique and being a non-equilibrium process it introduces crystalline disorder or radiation damage. Often this radiation damage may be unwanted and is removed by an annealing cycle, but frequently it may prove beneficial. Ion beam mixing is an interesting application of ion implantation where radiation damage can be used in fabricating and modifying material characteristics. This approach is particularly interested in creating stable compounds, durable imitation alloys, and super-saturated alloys. Also, it has the potential to improve the wear or corrosion resistance of metals. In semiconductors, IBM is utilized as a method for combining contacts, metal layer with a semiconductor for preparation of electrical, and it has been demonstrated to be useful for dispersal of impurities prior to film growth.

For the aims of present study, two groups of $TiO_2/SiO_2/Si$ structures with different layer thickness were surveyed. Mixing of the TiO_2/SiO_2 systems was induced by implantation the samples with four different species of noble ions Ne^+, Ar^+, Kr^+ and Xe^+ at four different energies of 100, 150, 200 and 250 keV. For each implantation, the fluence of the incident ion beam was fixed at 3×10^{16} (ions/cm^2). The noble gas ions were used due to they would not produce any chemical binding with the target atoms during interaction, in this way the samples only modified in physical structure. With these species of ions, the energy was chosen so that the ions interact with the atoms in samples at both before and beyond the TiO_2/SiO_2 interface.

2.2. Rutherford Backscattering Spectrometry (RBS) method.

In this work, the RBS experiments were carried out using ion beams accelerated by a Van de Graff accelerator at the EG-5 group, Frank Laboratory of Neutron Physics, JINR, Dubna, Russia. After acceleration process, the energetic ions pass through a magnet system for changing the beam direction from perpendicular to parallel with the floor surface. The beam is collimated to a small divergence angle at the target. The beam line pressure is about $l0^6$ Torr, connected with the target chamber located at the IBA experimental hall. Just before entering the chamber the beam spot has a diameter of nearly 5 mm. In the target chamber, the samples are putted on a holder that can keep four samples at the same time. The holder is designed to connect to a sensitive current integrator for monitoring the beam current. During bombardment, the backscattered particles are collected by a surface barrier detector placed in the chamber according to IBM geometry, in which, α is incident angle, and θ is scattering angle. The exit angle β is simply given by $\beta = |180^0 - \alpha - \theta|$. In the RBS experiment for analysis of $TiO_2/SiO_2/Si$ samples, a He^+ ion beam of 1.5 MeV was used.

2.3. Ellipsometry Spectroscopy (ES) method

In the present study, the ES experiments were conducted at the Institute of Electron Technology in Warsaw, Poland using the rotating-analyzer ellipsometer (RAE). The ellipse of the angles Ψ (λ) and Δ (λ) was measured with the light wavelength from 250 nm to 1100 nm, with the step of 1 nm at six different incident angles (i.e., the angle between direction of incident light beam and the normal of the sample surface), namely 70.0^0, 72.0^0, 74.0^0, 76.0^0 78.0^0, and 80.0^0. Once all these SE experiments had done, all the measured angles Ψ (λ) and Δ (λ) were used as input to calculate the spectra of Ψ (λ) and Δ (λ) using the Multiple-angle-of-incidence Ellipsometry (MAIE) method. In order to analyze the optical parameters of the irradiated $TiO_2/SiO_2/Si$ systems, a four-layer optical model was constructed. It consists of a Si substrate, a SiO_2 layer, TiO_2 layer, and an interface layer between SiO_2 and TiO_2. It was assumed that all layers are homogeneous, and the boundaries between the materials are sharp. The thickness, and concentration of the compounds of the material layers are free parameters, whose values were determined by fitting to the experimental Ψ (λ) and Δ (λ) spectra. Knowing the values of all the parameter models, the refractive index n, and extinction coefficient k, of the investigated samples were deduced using the effective medium approximation (EMA).

2.4. X-ray Photoelectron Spectroscopy (XPS) method.

In a XPS instrument, a sample is illuminated by low-energy X-rays to activate the photoelectric effect, the atoms of the surface thus excited by the electrons. The energy spectrum of photoelectric electrons is determined by the high-resolution electron spectrometer. Photovoltaic emission provides information about electron binding energy, chemical state, electronic state and quantitative composition of compounds. The recording and measurement of the kinetic energy of the excited photoelectric electron allows to determine their binding energy from known X-ray energy. Spectra measured include peaks corresponding to the electronic energy levels of the material. In this work, XPS method was used to study experimentally influence of changes in chemical composition induced by ion irradiation on mixing amount of TiO_2/SiO_2 systems as function of ion energy. XPS spectra were recorded in the energy range of 450 eV - 462 eV, this energy range represents the binding energy of the electrons Ti 2p.

CHAPTER 3
INFLUENCE OF ION ENERGY AND MASS ON MIXING OF TIO_2/SIO_2 STRUCTURES WITH DIFFERENT THICKNESS

In this chapter, variation in structural properties $TiO_2/SiO_2/Si$ systems induced by noble gas ion irradiation will be investigated using RBS method. The mixing process at the TiO_2/SiO_2 interface is described by shifting of borders associated to elements in RBS spectra. Mixing amount and direction are determined by changes in thickness of TiO_2 and TiO_2/SiO_2 transition layers. The mixing behavior will be investigated as a function of energy and mass of the incident ions for different thicknesses of TiO_2 and SiO_2 thin films.

3.1. Characterization of samples and the mixing process.

Regarding modification of the irradiated $TiO_2/SiO_2/Si$ structures, the RBS spectra of the thinner-layer samples (group 1) irradiated with Kr^+ ions of 100, 150, 200, and 250 keV as well as that of the virgin one were investigated. The presence of O and Ti at the near surface layer of the investigated $TiO_2/SiO_2/Si$ samples is indicated in Fig.3.1 by vertical arrows pointing to the high-energy edges of the corresponding peaks (also known as kinetic borders) at 530 and 1100 keV, respectively. In Fig.3.1, the presence of Si in the substrate and SiO_2 layers is marked by inclined arrows at the energy edges of 770 and 830 keV, respectively. The band at the energy between 370 and 530 keV indicates the He^+ ions backscattered from O in both TiO_2 and SiO_2 layers. Whereas, the presence of Kr atoms in the irradiated samples is noticed by an inclined arrow

pointing to the high-energy borders of the corresponding peaks at around 1225 keV. The implantation of Kr^+ ions caused a decrease in concentrations of O and Si, which is associated with a significant reduction in the yields of backscattered He^+ ions corresponding to O and Si nearly the energy of 485 and 800 keV, respectively. Obviously, there was no Kr peak in the RBS spectrum of the non-irradiated TiO_2/SiO_2 sample. Meanwhile, the Kr peaks of irradiated samples had a shift with growing ion energy. This shift can be attributed partially to the variation of Kr distribution that contribute to changes in TiO_2, SiO_2 layer thicknesses as well as mixing amount between these materials.

Focusing on the atomic mixing process, which is responsible for the broadening of the implanted TiO_2/SiO_2 transition layers, the measured RBS spectra are kept to be examined in extensive detail. As the implanting ion energy increases, a shift toward the higher energy region of the low-energy edges indicating the appearance of Ti in the TiO_2 layer was observed. This is an indication for the expansion of the mixed layer toward the sample surface, i.e., the outward mixing. The influence of ion irradiation on mixing of TiO_2/SiO_2 thus can be examined by surveying the full-width at half-maximum (FWHM) of the corresponding Ti Gaussian peaks in RBS spectra. As shown in Fig.3.1, these Ti peaks are well separated from the others, the surveyed FWHMs therefore do not sustain the uncertainty due to peak superposition.

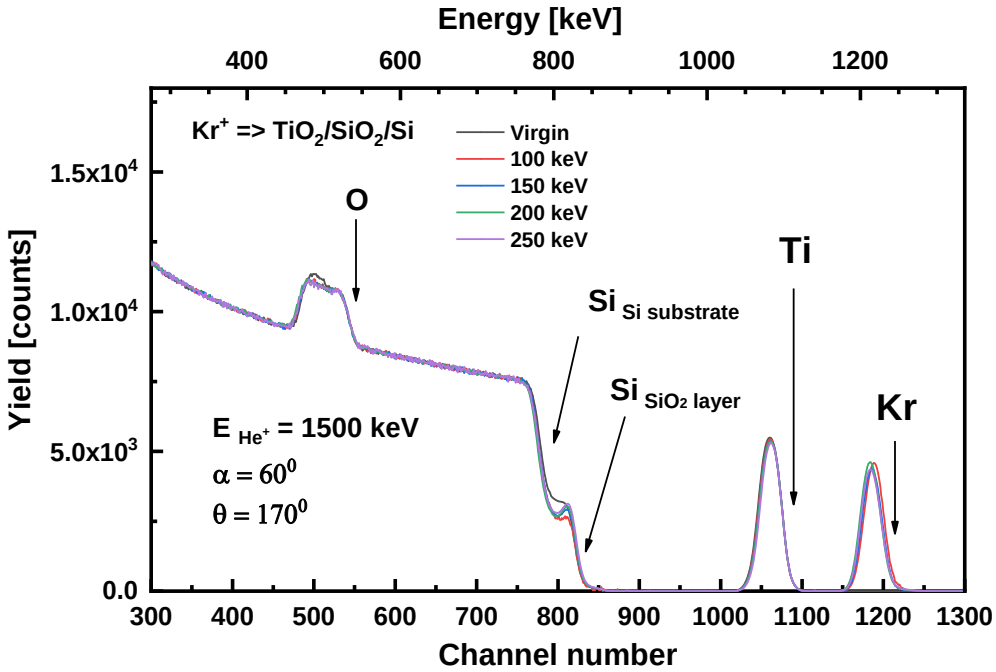

Fig.3.1. The RBS spectra that were collected from the thinner-layer samples (group 1) un-implanted and implanted with Kr^+ ions at different energies.

It is worth to mention that a study on role of expanding SiO_2 layers in the mixing of a Kr-implanted Al_2O_3/SiO_2 system has been pointed out by Galuska. However, in the present work, the variation of SiO_2 layer thicknesses simultaneously depends on the mixing processes occurring at both TiO_2/SiO_2 and SiO_2/Si interfaces. This situation is immensely complicated, and it has not been discussed. In this thesis, the difference between the FWHM, denoted as Δ(FWHM), of Ti peaks corresponding to the virgin TiO_2/SiO_2, and the samples irradiated with Ne, Ar, Kr and Xe at energies of 100, 150, 200, and 250 keV are examined. This is the first approach to evaluate the dependence of the mixing degree at the TiO_2/SiO_2 interface on the implanting ion energy.

3.2. Dependence of mixing degree on energy of incident ions.

Figure 3.2 shows the variation of Δ(FWHM) for Ti peaks in the RBS spectra collected from the samples before and after implantation with Ne^+, Ar^+, Kr^+, and Xe^+ ions as the function of ion energy. In general, FWHM of Ti peaks of the implanted samples decreases compared to that of the virgin one. Decreasing in FWHM indicates a reduction in concentration of Ti at the bottom of TiO_2 layers. It was noticed that sputtering phenomenon could be ignored due to their paltry amount, thus lessening in Ti concentration are caused only by the atoms that moved towards the Si substrate (inward displacement). This leads to narrowing of the TiO_2 layers and thus a broadening of the TiO_2/SiO_2 transition layer towards surface of the samples (outward mixing). With growing ion energy, FWHM reduced for the samples implanted by the Ne^+, Ar^+, and Kr^+ ions. In the energy range of 100 – 250 keV, FWHM drops from -15.6% to -18.9%; -13.0 % to -14.1 % and -1.7% to -6.8% for samples implanted by Ne^+, Ar^+, and Kr^+ ions, respectively. However, FWHM rises from -29.23% to -24.10% for Xe^+ ion irradiation.

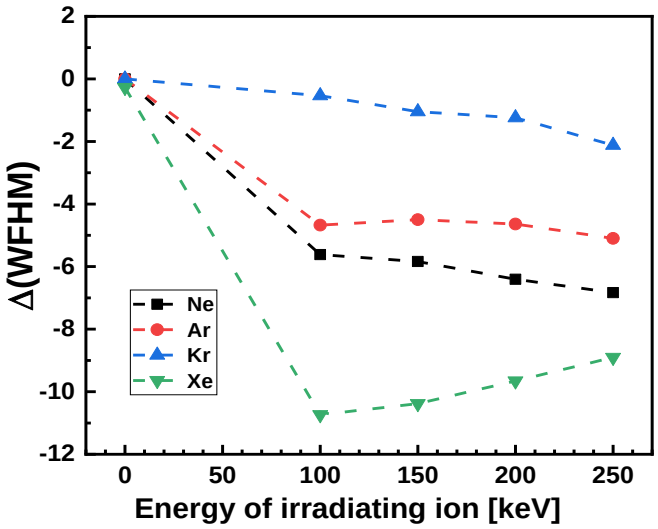

Fig.3.2. The variation of Δ(FWHM) of Ti peaks from RBS spectra as a function of Ne^+, Ar^+, Kr^+, and Xe^+ ions energy.

In a mixing study of A.M. Ibrahim for Bi/Sb system, surveying variation of *Δ(FWHM)* values shown that the mixing proceeds faster as the energy increases to 80 keV, then reduces slowly with ion energy. The enhancement in mixing amount indicated expending of the over-layer towards the substrate due to the inward displacement. In the present study, however, a decrease in the FWHM of implanted samples compare with that of the virgin one associated with outward mixing. For TiO_2/SiO_2 system, the atomic transportation becomes complex because of the existence of oxygen in the mixed area from both materials. Moreover, due to existence of initial transition layers between TiO_2 and SiO_2, the thickness of the mixed areas after ion irradiation will be modified in both inward and outward directions. Accordingly, the variation of the TiO_2 layer thickness, represented by the Δ(FWHM), does not completely quantify the mixing process.

To better inspect the variation of the mixing degree concerning inward displacement as a function of irradiating ion energy, we calculated the relative thickness r_t, which is defined by

$$r_t = (t_{im} - t_{vir})/t_{vir}$$

where t_{vir} and t_{im} are the thickness of the layers before and after implantation, respectively. It recalls that t_{vir} and t_{im} were determined based on the experimental RBS profiles. The role of the ion energy in the mixing amount was examined by surveying r_t at different energies from 100 to 250 keV. An increase in relative thickness with ion irradiation energy is seen in Fig.3.3 for all ions species. Generally, this indicates that the energy transferred to recoil atoms in the transition layer by incident ions is proportional to their initial energy. Because higher-energy ions displaced atoms travel longer through the samples, the transition layer thickness expands. This effect agrees with Sigmund's conclusion that the noticeable increase in mixing rates occurs at a fixed depth with increasing irradiating ion energy. However, for oxide/oxide systems, other contributions in mixing process should be discussed in more detailed.

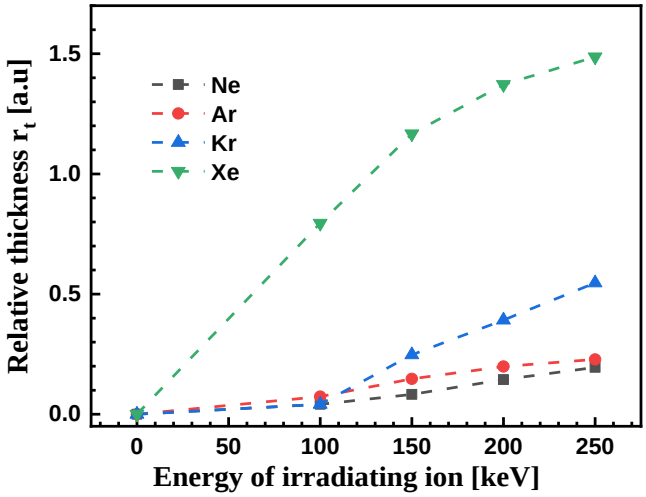

Fig.3.3. The variation of the relative thickness r_t as a function of ion energy (RBS calculation).

The energy transferred to recoil atoms could be considered as nuclear energy loss of ions. Using SRIM simulation, both nuclear and electronic energy loss (S_n and S_e) were obtained for interpretation (Table 1). In the low energy range (100-250 keV), nuclear energy loss shown to be dominant i.e., ions lose their energy almost via interaction with nuclei more than that of electrons. With the rising of energy, S_n tends to decrease slowly for Ne^+ and Ar^+ ions leading to fewer effects on the mixed layers compared with that of Kr^+ and Xe^+, whose energy to recoils increase strongly with growing of ion energy. It suggests that changes in mixing amount not only depend on ion energy loss, this is the reason why mixing amount is not simple function of ion energy. For better understand, the mixing behavior concerning to target damages will be inspected below.

From the RBS experiments, it has been observed that the thickness of the TiO_2/SiO_2 transition layers is inversely proportional to the Δ(FWHM) of the Ti peak in the RBS spectrum. Based on the depth profiles of elements determined by RBS, the thickness of the mixed layers after irradiation increases 7% for 100-Kev Ne to 149% for 250 KeV Xe compared with that of the virgin sample. This percentage associated with the layer thickness from 1 to 28.8 nm. In the meantime, decreasing of $\Delta(FWHM)$ varies from 1.7% for 100 keV Kr to 29.2% for 100 keV Xe associating with 0.3 to 4.1 nm in layer thickness. Contribution of decreasing FWHM to mixing thus seem to be not significant in comparison to rising relative thickness of transition layers. The cascade mixing process is responsible for broadening of mixed are, occurs towards both the substrate and the surface of the samples. Nevertheless, the expansion toward the substrate, namely the inward displacement of Ti atoms into the SiO_2 layer, is dominant. The mixing degree is not proportional to the damage amount, whereas the ion energy transfers to the target atoms create deeper damage plays a crucial role in broadening the TiO_2/SiO_2 mixed area.

Table 1. The interaction parameters calculated at TiO_2/SiO_2 mixed area for the samples in group 1 implanted by ions at different energies, using SRIM simulation.

Ion	Energy [keV]	Ion range [nm]	Number of ion across transition layer [ions/cm^2]	Displacement per ion	Vacancy per ion	Energy loss [keV/ion]	
						Nuclear (S_n)	Electronic (S_e)
Ne	100	2027.3	1.4E+14	41.1	40.0	3.0	3.0
	150	3395.3	5.9E+13	34.0	33.1	2.3	4.9
	200	4232.1	3.5E+13	31.9	31.1	2.2	6.0
	250	5417.7	2.5E+13	30.3	29.5	2.0	7.2
Ar	100	975.5	9.9E+14	157.2	153.3	10.8	4.8
	150	1664.0	2.9E+14	122.8	119.8	9.3	6.5
	200	2237.8	1.2E+14	102.6	100.1	8.1	7.5
	250	2811.6	6.1E+13	88.6	86.4	7.3	8.2
Kr	100	552.0	2.2E+15	259.2	253.4	17.0	2.3
	150	795.6	9.6E+14	271.7	265.0	18.0	3.2
	200	1036.0	4.8E+14	276.1	269.3	20.6	4.3
	250	1398.6	2.3E+14	246.7	240.4	19.6	4.1
Xe	100	454.3	8.1E+15	548.2	534.3	23.5	1.9
	150	617.9	3.2E+15	610.3	595.3	33.2	3.4
	200	741.5	1.2E+15	573.0	558.8	37.4	4.6
	250	988.7	5.0E+14	532.4	519.1	38.9	5.6

3.3. Study on mixing of TiO_2/SiO_2 systems with different thicknesses.

In order to investigate influence of layer thickness on mixing amount, the thicker-layer TiO_2/SiO_2 systems (group 2) were measured. Due to the structural differences of the samples implanted with Xe ions in 2 groups compared to the rest, these samples were not used for the studied purpose. Mixing process thus only investigated by the samples implanted with Ne^+, Ar^+ and Kr^+ ions. The mixing amount will be compared by mean of the new concept of defect level – displacement per atom (DPA) according to the variation in incident ion energy. However, the first survey is based on the experimental and simulation parameters obtained by RBS and SRIM as given.

The variation in relative thickness of TiO_2/SiO_2 mixed layers as a function of ion energy for the samples in groups 1 and 2 are shown in Figs.3.4a and b, respectively. Generally, thickness of the transition layers for 2 groups increased linearly with the ion energy. In case the samples implanted by the same ion species, faster rising r_t was observed for the samples in the group 1. Varying of r_t values were approximated using the fitting line as a linear function: $r_t(E) = a \times E + b$. Where the parameters a and b are known as the slope and r_t-intercept of the equation respectively, E indicates to the energy of implanted ions. Table 1 shows slope values of the linear fitting function for increasing of r_t for all investigated samples. It is clear that faster increasing in transition layer thickness of samples in group 2 corresponds to the higher slope parameters of

fitting lines. In other word, mixing rate is greater for the thinner initial TiO_2 layers. It should be kept in mind that difference in thickness of TiO_2 and SiO_2 layers leads to deviation of initial transition area for the samples between two groups. An average deviation about 15 nm was found based on RBS depth profile. Thus, although r_t is a good representation mixing amount for the samples in individual of two groups, it does not show the correlation between them.

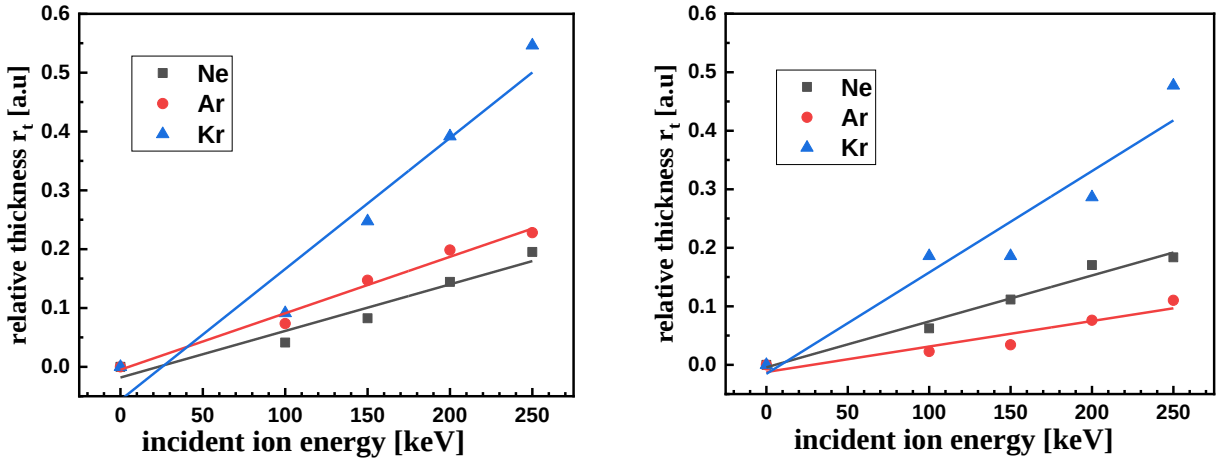

Fig.3.4. Variation of relative thickness r_t as a function of ion energy for the samples in group 1 (a) and group 2 (b).

Table 2. The slope values of the linear fitting function for increasing of r_t for the samples in group 1 and 2.

Ions	**Slope *a***	
	Group 1	Group 2
Ne	7.9E-4 ± 1.1E-4	7.8E-4 ± 0.7E-4
Ar	9.6E-4 ± 0.7E-4	4.3E-4 ± 0.8E-4
Kr	22.0E-4 ± 3.0E-4	17.0E-4 ± 3.0E-4

Indeed, while the slope values for thinner-layer samples (group 1) are higher, the simulation parameters suggest the contrary. The total loss energy, number of ion across transition layer, and defects density show higher values for samples of group 2 due to thicker initial transition layer. Moreover, the measured defects (in unit atom/cm^3) only explains the difference in term of defect density for layers of same thickness. Therefore, for a better comparison the parameter displacement per atoms (DPA), which refers damage level of the sample structure, was calculated for a thickness of 20 nm under bottom of the TiO_2 layer for both groups.

Table 3 shows the DPA of Ar, Kr and Ne ions at different energies for the samples in both groups. Where the values in the table were calculated for a thickness of 20 nm under bottom of the TiO_2 layer for both groups. It is clear

that DPA for group 2 is higher than groups 1 in all cases. Within interaction of ions with atoms, when an ion transferred to the PKA high enough energy, E >> E_d, the PKA will be able to continue the PKA process to displace other atoms of the crystal, creating secondary recoil atom displacement. The lattice atom in collision receives energy that is less than the displacement threshold energy, the atom can be knocked out of its position in the crystal but will not be displaced. DPA thus refers displacements that produced by PKA directly. The DPA values for group 2 larger than group 1 means that there are more displaced atoms produced by PKA in transition area for thicker-TiO_2 samples. This shows greater reactivity level of atoms with ions under the thicker TiO_2 layer creating more defects, lead to higher mixing amount as a consequence.

Table 3. DPA calculated for a thickness of 20 nm under bottom of the TiO_2 layer for the samples implanted by Ar, Kr, Ne at different energies.

Energy [keV]	**Ar**		**Kr**		**Ne**	
	G2	G1	G2	G1	G2	G1
100	100.9	82.6	181.4	170.2	30.7	26.3
150	85.1	70.1	201.4	171.6	23.5	19.0
200	71.0	59.8	204.4	164.0	19.2	15.9
250	62.2	53.4	190.9	145.4	15.3	14.1

It was noticed that with thicker TiO_2 layers, the ions travel longer distances and collide with more atoms along the inward path. Thus, the ions lose more energy in the TiO_2 layer of samples in group 2. The larger energy loss of ions could make a misleading that the remaining energy create less damage in transition area for thicker-layer samples. However, the DPA at the 20-nm mixed layers show greater values for group 2 than that of group 1. That means, despite lower energies, ions produced more damages at mixed layers. This effect could be taken into account by the main role of correlation between ion range, number of interacting ions and transition area position Table 4). Therefore, for the investigated TiO_2 thickness below 30 nm, higher DPA refers to more damage as well as mixing for thicker layers. Although the simulation parameters are insufficient to compare the mixing in this case, a combination with calculated DPAs allowed to interpret variation of TiO_2/SiO_2 mixed layers with deviation in layer thickness in terms of target damage and atomic transportation.

Table 4. The interaction parameters calculated using SRIM simulation at TiO_2/SiO_2 mixed area for the samples in group 2 implanted by ions at different energies.

Ion	Energy [keV]	Ion range [nm]	Number of ion across transition layer [ions/cm^2]	Displacement per ion	Vacancy per ion	Energy loss [keV/ion]	
						Nuclear (S_n)	Electronic (S_e)
Ne	100	2027.3	5.9E+14	92.8	90.9	6.4	7.7
	150	3395.3	1.9E+14	70.5	69.1	5.0	9.3
	200	4232.1	1.0E+14	68.1	66.7	4.8	11.8
	250	5417.7	7.4E+13	70.3	68.8	4.8	15.5
Ar	100	975.5	4.2E+15	310.7	304.0	21.1	7.7
	150	1664.0	1.2E+15	248.0	243.0	18.9	11.2
	200	2237.8	4.5E+14	204.5	200.2	16.4	13.4
	250	2811.6	2.2E+14	175.2	171.6	14.6	14.8
Kr	100	552.0	1.6E+16	641.3	625.3	30.8	3.3
	150	795.6	6.9E+15	731.8	716.0	45.5	6.6
	200	1036.0	2.9E+15	681.5	667.0	49.2	9.0
	250	1398.6	1.3E+15	614.1	600.9	48.6	9.4
Xe	100	454.3	1.3E+16	394.6	383.1	18.4	1.0
	150	617.9	6.4E+15	523.7	513.3	29.2	2.5
	200	741.5	2.7E+15	525.1	515.3	36.4	3.9
	250	988.7	1.3E+15	501.0	491.0	39.6	4.9

CHAPTER 4
INFLUENCE OF ION ENERGY ON CHEMICAL AND OPTICAL PROPERTIES OF THE $TIO_2/SIO_2/SI$ SYSTEMS

4.1. Influence of the ion energy on chemical composition of TiO_2 near surface layers, and its effect to mixing of TiO_2/SiO_2 systems.

The results that obtained from XPS for the layer about 10 nm, thus could be considered similarly for whole of TiO_2 film. Generally, it is useful for surveys of unknown contamination. It was found that higher valence oxidation state species has electrons bound with higher energy compared with more reduced state but in atoms with same formal valence state, the energy bonds increases with electronegativity of neighbouring atoms. Using the XPS method, the chemical compositions of the near surface layers of TiO_2/SiO_2 bilayers were investigated. Fig.4.1 shows the XPS spectra of Ti 2p (Ti $2p_{3/2}$

and Ti $2p_{1/2}$) electrons in the region from 450.0 eV to 462.0 eV. The spectra were collected on the samples that were before and after implantation with Ne^+ ions at different energies 100, 150, 200, 250 keV. It is known that the bands in this region can be assigned to Ti 2p electrons. They refer to Ti atoms and the chemical compounds TiO, Ti_2O_3 and TiO_2. The local maxima in these bands are 453.86 eV, 455.34 eV 457.13 eV and 458.66 eV, they were related to the bands of Ti $2p_{3/2}$ Ti, TiO, Ti_2O_3 and TiO_2 respectively (Fig.4.1a).

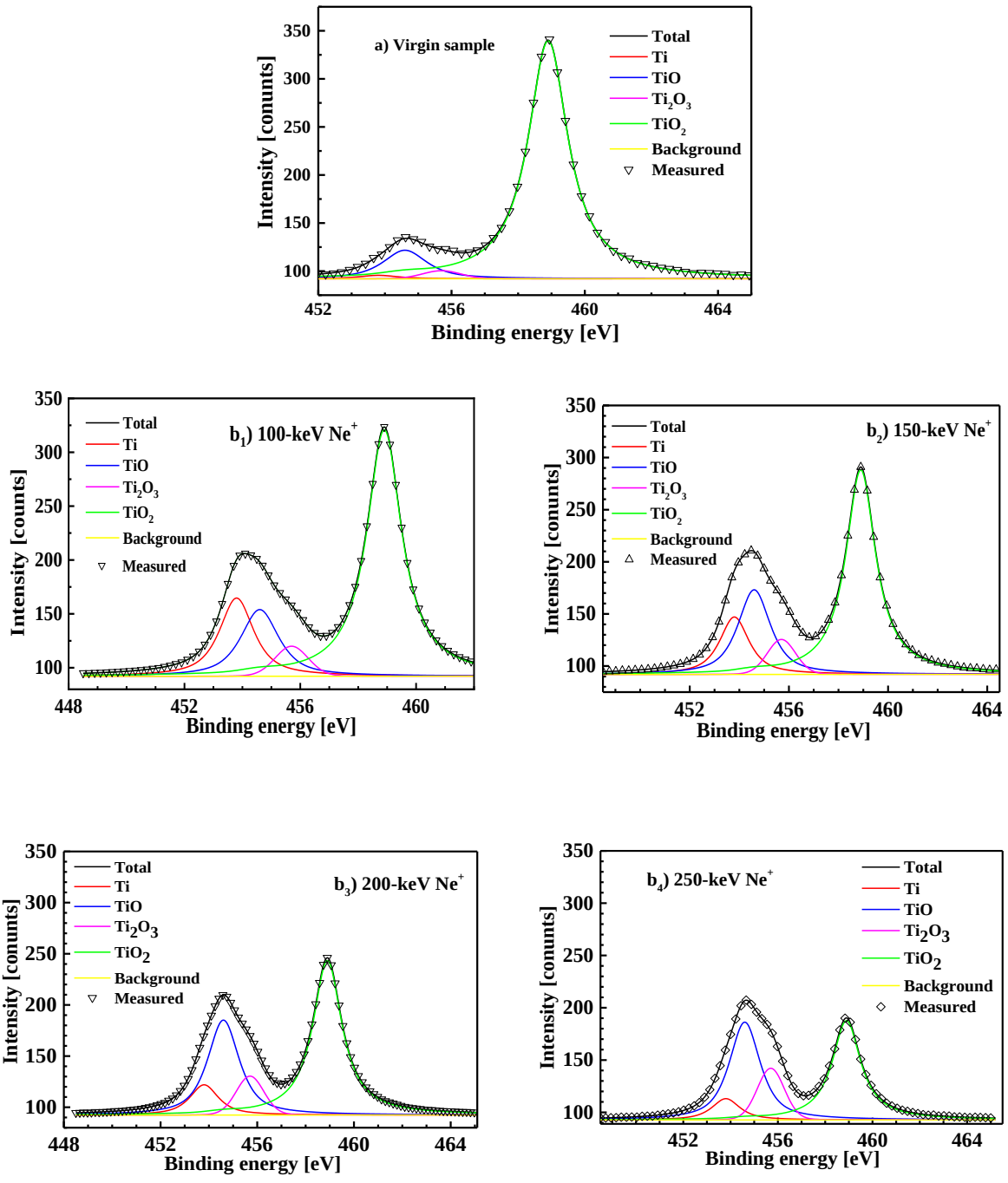

Fig.4.1. *XPS spectra of Ti 2p bands for the samples that were before (a) and after implanted with Ne^+ ions at different energies of 100 (b1), 150 (b2), 200 (b3) and 250 (b4) keV*

The XPS spectra obtained from the virgin and implanted samples have different shapes and the intensity of the bands changes (Fig.4.1b_1-b_4). This effect can be related to the changing concentration of the compositions Ti, TiO, Ti_2O_3 and TiO_2. As can be seen that the intensity of the Ti and TiO_2 bands decreases, however, TiO and Ti_2O_3 increases during the binding energy increase from 100 to 250 keV. These results indicate that the chemical bonding states of titanium were TiO, at the surface, various titanium oxides below the surface and a mixture of both metal and oxides in the interior. Fig.4.2 shows the changes of relative concentration of the compounds as a function of energy of Ne^+ ions. It was assumed that the concentration of compounds in the layers is proportional to the surface area of the bands obtained after deconvolution. The obtained results show that the relative concentrations of TiO, Ti_2O_3 (Fig.4.2a) increased while the relative concentrations of Ti and TiO_2 (Figs.4.2a and b) decreased with the projectile energy.

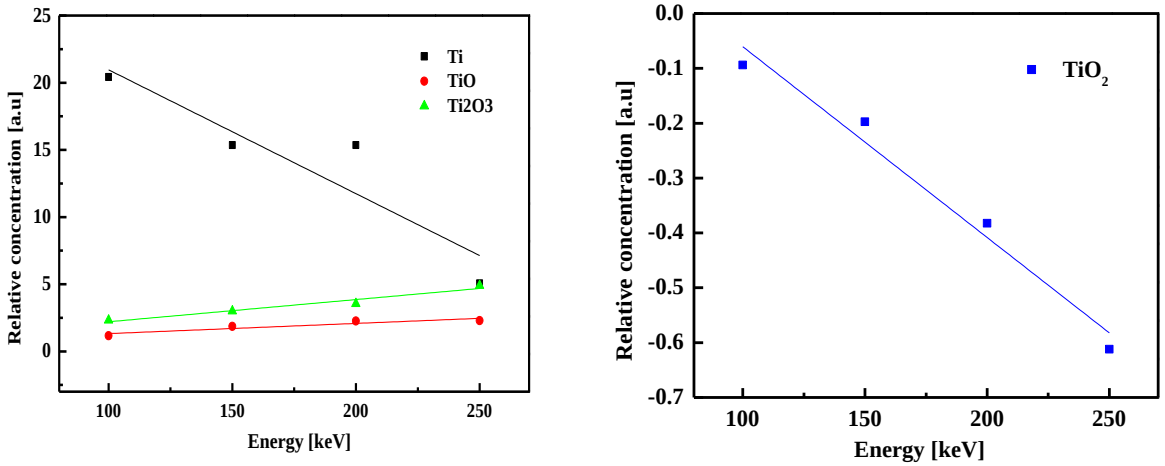

Fig.4.2. The variation relative concentration of the Ti, TiO, Ti_2O_3 (left) and TiO_2 (right) as a function of the irradiating ion energy.

Using SRIM code, a simulation for loss energy of ion in different chemical compounds were performed. Thickness of the investigated layers was chosen so that at this thickness (around 10 nm) the XPS results possess good sensitivity. Fig.4.3 shows loss energy of Ne ions as a function of ion energy in different compound of TiO_2, Ti, TiO and Ti_2O_3. It was observed that for compounds, loss energy linearly decreased with energy of implanted ions. The ions lost their energy highest in TiO_2, following by Ti, TiO and Ti_2O_3. As determined by XPS method, concentration of TiO_2 decrease when energy of implanted ions increased lead to decreasing of loss energy in TiO_2 near surface layer. Moreover, Ti, TiO, Ti_2O_3 just occupy a small percentage in TiO_2 film, that means decreasing of loss energy in TiO_2 refers the strongest increasing of deposited energy in sublayers and the transition layers compared with that of Ti, TiO, Ti_2O_3. Thus energy deposited at interface of TiO_2/SiO_2 depends not only on mass, energy of ions, thickness of TiO_2 layer but also on difference in

chemical compound as well as variation in their concentration. Decreasing concentration of TiO_2 after irradiation could be considered as one of the reasons that influent to mixing process at TiO_2/SiO_2 interface induced by ion beam. This effect lead to increasing of deposited energy which refers increasing amount of mixing or broadening of transition layers with energy of implanted ions which was also determined by RBS method.

4.2. The optical property of the TiO_2/SiO_2 mixed layers obtained by Spectroscopy Ellipsometry.

4.2.1. Variation of refractive index (n) and extinction coefficient (k) with ion energy

Two important optical properties, namely the refractive index *n* and extinction coefficient *k* of the transition layers for all investigated TiO_2/SiO_2 samples, were determined using the VASE ellipsometer software. The obtained results are plotted in Fig.4.3. It turns out that the variation of the refractive index and extinction coefficient as a function of wavelength does not depend on the irradiating Xe^+ ion energy. The refractive index of all investigated samples increases up to λ = 300 nm and then decreases. Similar behavior is found with the extinction coefficient except that the maximum is reached earlier at 260 nm. The absolute values of the refractive index and extinction coefficient indicate that these effects are caused by the structural defects and the changes in the element composition of the transition layer. It can also be seen in Fig.4.3 that at any arbitrary wavelength, the virgin sample's refractive index and extinction coefficient are the lowest. For irradiated samples, these coefficients rise with Xe^+ ion energy up to 200 keV and then suddenly drop for 250 keV. The atom displacements produced by the incident Xe^+ ions lead to the higher absorption of the TiO_2-SiO_2 system and change the light propagation in the mixed layers. However, for the irradiating ion energy of 250 keV, the number of displaced atoms decreases, associating with a reduction of the TiO_2 component in the mixed layer. This phenomenon probably explains the sudden decrease of n and k values shown in Fig.4.3. Moreover, the light absorption could also be affected by the presence of Xe atoms, which remains in the studied system, especially in the mixed layer. The projected range of 250-keV Xe^+ ions is far beyond the interface of TiO_2/SiO_2, but for 100-keV ions, it becomes very similar to the thickness of the top TiO_2 layer. Therefore, the lack of Xe atoms in transition layers and a smaller number of atom displacements in the sample irradiated with 250-keV ions are the probable reasons for the low values of *n* and *k* of this sample, which are almost the same as those of the sample irradiated with 100-keV Xe^+
ions.

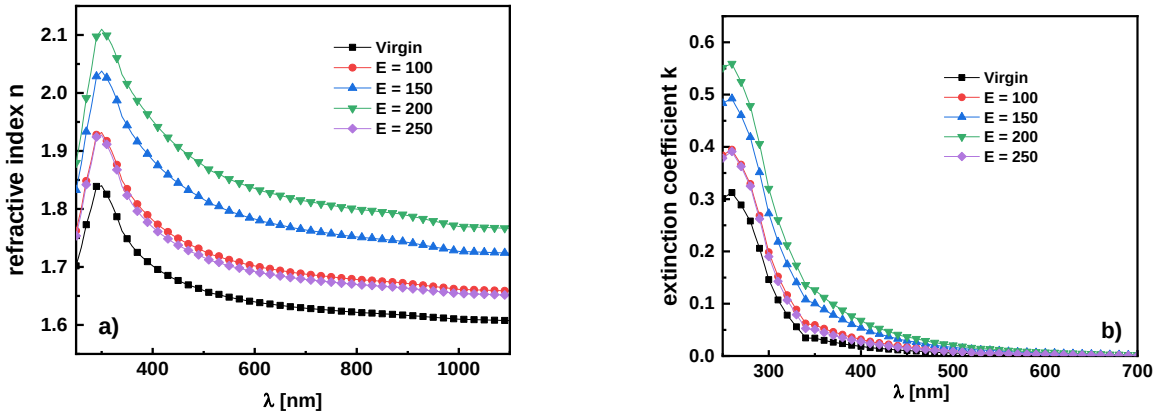

Fig.4.3. The refractive index *n* (a) and extinction coefficient *k* (b) for the transition layers of un-irradiated and irradiated TiO_2/SiO_2 systems as a function of wavelength.

4.2.2. Variation of optical energy gap (E_g) of TiO_2/SiO_2 mixed area with ion energy

A four-layer optical model which consists of a Si substrate, a SiO_2 layer, a TiO_2 layer, an interface layer between TiO_2 and SiO_2 was built to analyze the SE spectra. Each layer of the model has several fitting variables such as thickness and optical dispersion model parameters. A value of the goodness of fit, which quantifies how well the data generated by the optical model fit the experimental data, is derived from the root mean squared error (MSE). The thickness, components and optical constants of layers were extracted from experimental ES data using the software of the VASE ellipsometer. Figure 4.4 shows the model used to simulate the virgin TiO_2/SiO_2 sample. As mentioned that all the layers are assumed to be homogeneous with sharp boundaries. The transition layer between TiO_2 and SiO_2 layers was described as a mixture of TiO_2 and SiO_2 compounds.

3	*TiO_2 layer*	*30.8 nm*
2	*TiO_2/SiO_2 transition layer*	*3.0 nm*
1	*SiO_2 layer*	*144.1 nm*
0	*Si substrate*	*1 mm*

Fig.4.4. The model used in the MAIE calculations.

For getting the information about the structure and bandgap, optical absorption can be regarded as an effective approach. The absorption coefficient, which quantifies the amount of light absorbed by a medium, is defined by the fraction of incident radiation absorbed per thickness of the absorber. From Figs.4.5a and b, the optical energy gap is determined by plotting Tauc equation

and taking the extrapolation of the linear portion of the $(\alpha h\nu)^2$ and $(\alpha h\nu)^{1/2}$ as a function of $(h\nu)$ curve to (α=0), respectively. The extracted E_g values of the five samples which are virgin, and implanted by Xe 100, 150, 200 and 250 keV are shown in Fig.4.6. It is evident that the mixed layers of the implanted samples have smaller E_g compare with that of the virgin one. E_g decrease with growing of ion energy up to 200 keV, and then increase with ion energy of 250 keV.

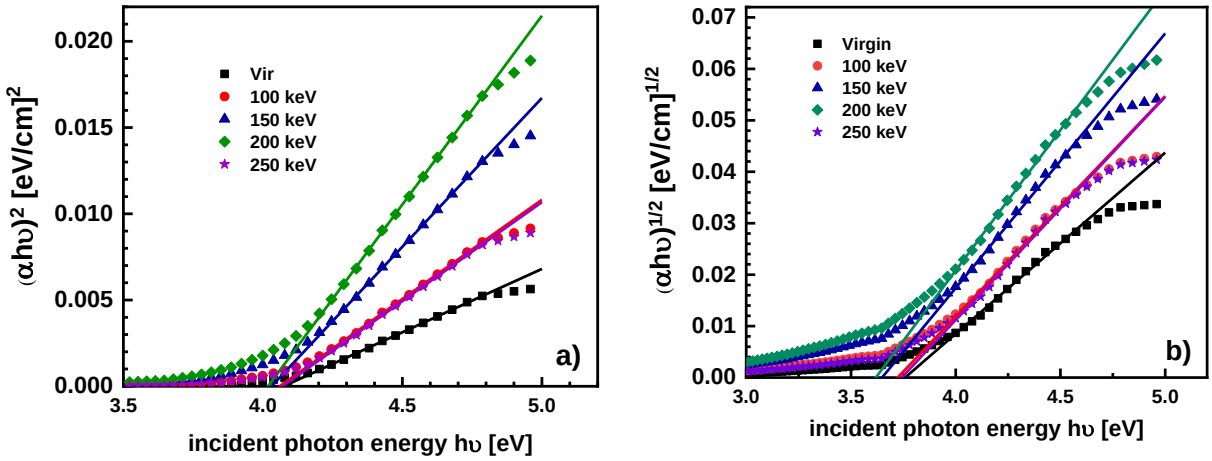

Fig.4.5. Plot of $(\alpha h\nu)^2$ (a) and $(\alpha h\nu)^{1/2}$ (b) vs. photon energy, the bandgap energy is deduced from the extrapolation of the straight line to $(\alpha h\nu)^2 = 0$ and $(\alpha h\nu)^{1/2} = 0$.

It should be noted that the thickness of the films increases the absorbance due to scattering losses. It is clear that there are large variations in the optical edge of the films with an increase in thickness. The thickness of the film causes a shift in the optical absorption edge and therefore a change in the band structure of the films.

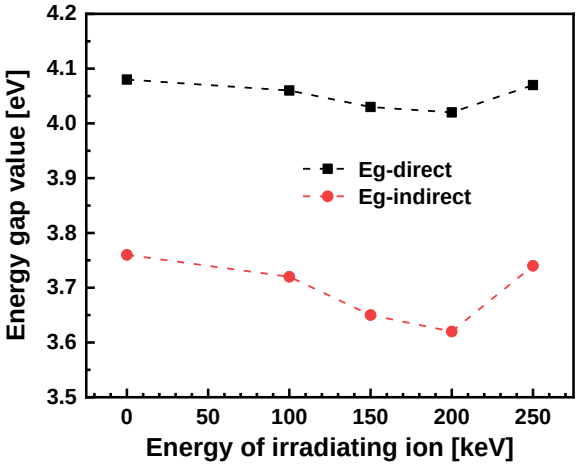

Fig.4.6. Energy gap values as a function of incident ion energy for Xe-implanted TiO_2/SiO_2 mixed layers.

It is found that the optical absorption edge varies with increasing ion energy. This confirms that the defects in thin films occur during the broadening of the films, unsaturated bonds can be produced as a result of an insufficient number of atoms.

These bonds are responsible for the formation of some defects in the films and these defects produce localized states in the films. Growing of defects enhances the width of localized states in the optical band gap; consequently, the optical absorption edge decreases with the reverse effect. The optical band gaps enhancement therefore can be attributed to the changes in mixed layer thickness and concentration of TiO_2 in this area due to variation of produced defects.

CONCLUSIONS AND FUTURE SCOPE

In the present dissertation, the ion-induced mixing of TiO_2/SiO_2 bilayers was characterized and quantified using RBS method. The oxide/oxide samples were irradiated by the noble gas ions Ne^+, Ar^+, Kr^+, and Xe^+ at four different energies of 100, 150, 200, and 250 keV. Mixing process is associated with shifting of the RBS spectra borders, thus the mixing amount has been usually determined by variation in FWHM of the peaks of over layers. This method, however, did not fully quantify mixing for the oxide/oxide systems. This work utilized evaluating the degree of variation in relative thickness of TiO_2/SiO_2 transition layers as a new approach to survey mixing amount. Broadening thickness of these mixed area was investigated as a function of ion energy and mass.

In the energy range of 100 - 250 keV, the interactions occur due to diffusion controlled by cascade mixing. With increasing ion energy, mixing amount enhances associating with changes in atomic transport process. The dependence of mixing on energy has been observed as a simple linear function for all ion species Ne^+, Ar^+, Kr^+, and Xe^+. Mixing degree is not proportional to the defect concentration, whereas the ion energy transfers to the target atoms creating deeper damage play a crucial role in broadening of TiO_2/SiO_2 mixed area, in other words, the inward mixing process is dominant. Since the heavier ions lose energy more intensively and are closer to the interface than the light ions, the mixing amount shows a strong dependence on ion mass.

The chemical compounds including Ti, TiO_2, TiO, and Ti_2O_3 for 10 nm thickness of un-irradiated and irradiated TiO_2 surface layers have been identified using XPS method. Concentration of TiO, Ti_2O_3 increase while concentrations of Ti and TiO_2 decrease with the growth of incident ion energy. Besides, energy loss of Ne ions linearly reduces with ion energy, and the ions lose most of their energy in TiO_2. Accordingly, reducing TiO_2 concentration, which enhances energy deposited at the TiO_2/SiO_2 mixed layers, is considered one of the reasons for mixing amount enhancement as also found by RBS method.

Using ES method, the thickness of layers, chemical compounds and optical parameters of the TiO_2/SiO_2 mixed layers before and after irradiation have been

obtained. The variation of the refractive index n and extinction coefficient (k) does not depend on the irradiation as a function of wavelength, while n and k values vary with ion energy. The n and k of the irradiated samples increase as the Xe^+ ion energy rises from 100 to 200 keV. At 250 keV, both these parameters decrease to almost the same as those corresponding to the energy of 100 keV. A similar relation has also been observed for changes in the optical energy gap of the TiO_2/SiO_2 mixed layers. These effects are attributed to changes in TiO_2 amount due to varying created defects concentration in mixed areas. It is worth mentioning that the calculating results for thickness of TiO_2/SiO_2 mixed layers obtained by ES and RBS methods are in good agreement.

The results of the present work are useful in extending the understanding influence of ions on an oxide/oxide material system. Although the experimental observations and the conclusions have been given, there are still restrictions. For the structural modification, in this thesis, we focus mainly on the kinetics transportation of ion-solid interactions within the mixing phenomena caused by low-energy ions. Some other effects such as amorphization, phase formation, or adhesion of layers have not been investigated. Thus, more detailed studies on these effects are recommended with a broader range of ion energy for both bilayer and multilayer systems. Also, the ion fluence dependence needs to be surveyed so that the mixing rate could be estimated. Regarding the material properties modification, for an ARC, refractive index should be constant over time, and absorption in materials at interfaces should remain as low as possible. In our work, the results obtained from the ES method thus predict a degradation for irradiated solar cells. However, conclusions cannot be reached due to some experimental limitations in the framework of the thesis. Therefore, determining variation of optical constants for the ARC system induced by ions, and how it affects to efficiency of the solar systems need to be considered in the forthcoming studies.

LIST OF PUBLICATIONS

1. **Tran Van Phuc**, M. Kulik, A. P. Kobzev, Le Hong Khiem, Study of MOS structures using nuclear analytical methods, Communications in Physics, Vol. 27, No. 4 (2017), pp. 279-289. https://doi.org/10.15625/0868-3166/27/4/10825

2. **T.V. Phuc**, M. Kulik, A. P. Kobzev, L. H. Khiem, Study of elemental depth distribution in the material $TiO_2/SiO_2/Si$ by Rutherford Backscattering Spectrometry (RBS), Communications in Physics, Vol. 29, No. 3SI (2019), pp. 393-400. http://dx.doi.org/10.15625/0868-3166/29/3/14328

3. **T.V. Phuc**, M. Kulik, D. Kołodyńska, L.H. Khiem, P.L. Tuan, J. Zuk, M. Turek,
Investigations of elemental depth distribution and chemical compositions in the $TiO_2/SiO_2/Si$ structures after ion irradiation, Surface & Coatings Technology, 387 (2020), 125494. http://dx.doi.org/10.1016/j.surfcoat.2020.125494

4. P.L. Tuan, M. Kulik, J. Nowicka-Scheibe, J. Żuk, P. Horodek, L.H. Khiem, **T.V. Phuc**, Nguyen Ngoc Anh, M. Turek, Investigations of chemical and atomic composition of native oxide layers covering SI GaAs implanted with Xe ions, Surface and Coatings Technology, Volume 394, 25 July (2020), 12587.
http://dx.doi.org/10.1016/j.surfcoat.2020.125871

5. **Tran Van Phuc**, Miroslaw Kulik, Le Hong Khiem, Afag Madadzada, Marcin Turek, Dorota Kołodyńska, Phan Luong Tuan, Nguyen Ngoc Anh, Mai Quynh Anh, Nguyen Van Tiep, Krzysztof Siemek, Variation of TiO_2/SiO_2 mixed layers induced by Xe^+ ion irradiation with energies from 100 to 250 keV, Materials Science and Engineering: B, Volume 277, (2022), 115566.
https://doi.org/10.1016/j.mseb.2021.115566

6. P.L. Tuan, M. Kulik, **T.V. Phuc**, A.I. Madadzada, T.Yu. Zelenyak, M. Turek, J. Zuk, C. Mita, A. Stanculescu, A.S. Doroshkevich, B. Jasinska, L.H. Khiem, N.N. Anh, N.T. Bao My, Pseudo-dielectric function spectra of the near surface layer of GaAs implanted with various fluence of Xe+ ions, Thin Solid Films 756 (2022) 139376. https://doi.org/10.1016/j.tsf.2022.139376

REFERENCES

[1] Schmidt, Bernd, Wetzig, Klaus, Ion Beams in Materials Processing and Analysis, Springer-Verlag Wien, 2013. http://dx.doi.org/10.1007/978-3-211-99356-9

[2] J.W. Nastasi and M. Mayer, 2007, Ion Beam Mixing, in Radiation Effects in Solids, NATO Science Series, Springer, Dordrecht.

[3] L.S. Hung, M. Nastasi, J. Gyulai, J.W. Mayer, Ion-induced amorphous and crystalline phase formation in Al/Ni, Al/Pd, and Al/Pt thin films, Applied Physics Letters 42, 672. https://doi.org/10.1063/1.94068.

[4] J.W. Mayer, B.Y. Tsaur, S.S. Lau, L.S. Hung, Ion-beam-induced reactions in metal-semiconductor and metal-metal thin film structures, Nuclear Instruments and Methods 182-183 (1981)1-13. https://doi.org/10.1016/0029-554X(81)90666-2.

[5] S. Balaji, S. Amirthapandian, B.K. Panigrahi, S. Kalavathi, G. Mangamma, A. Gupta, A.K Tyagi, Study of ion beam mixing in Pt/Co bilayer by ion beam analysis. Nuclear Instruments and Methods in Physics Research Section B: Beam Interactions with Materials and Atoms, 266(8), (2008) 1692–1696. https://doi.org/10.1016/j.nimb.2008.01.055.

[6] C. Palacio, A. Arranz, The application of ITTFA and ARXPS to study the ion beam mixing of metal/Si bilayers. Surface and Interface Analysis, 40(3-4), (2008) 676-682. https://doi.org/10.1002/sia.2683

[7] N. Benito, C. Palacio, Growth of Ti-O-Si mixed oxides by reactive ion-beam mixing of Ti/Si interfaces. Journal of Physics D: Applied Physics, 47(1), (2013) 015308. https://doi.org/10.1088/0022-3727/47/1/015308

[8] S. Dhar, P. Schaaf, N. Bibić, E. Hooker, M. Milosavljević, K.P. Lieb, Ion-beam mixing in Fe/Si bilayers by singly and highly charged ions: evolution of phases, spike mechanism and possible effects of the ion-charge state. Applied Physics A, 76(5), (2003) 773–780. https://doi.org/10.1007/s00339-002-2045-9

[9] S.K. Sinha, D.C. Kothari a, T. Som, V.N. Kulkarni, K.G.M. Nair, M. Natali, Effects of Ne and Ar ion bombardment on Fe/SiO_2 bi-layers studied using RBS, Nuclear Instruments and Methods in Physics Research B 170, (2000) 120–124. https://doi.org/10.1016/S0168-583X(00)00068-9.

[10] P. Sigmund and A. Gras-Marti, Theoretical aspects of atomic mixing by ion beams, NucI. Instrum. Methods, 182/183 (1981) 25-41. https://doi.org/10.1016/0029-554X(81)90668-6

[11] W.L. Johnson, Y.T. Cheng, M. Van Rossum and M.-A. Nicolet, When is thermodynamics relevant to ion-induced atomic rearrangements in metals?, NucL Instrum. Methods, B7/8 (1985) 657-665. https://doi.org/10.1016/0168-583X(85)90450-1

[12] Mazur, M., Wojcieszak, D., Domaradzki, J., Kaczmarek, D., Song, S., Placido, F., TiO_2/SiO_2 multilayer as an antireflective and protective coating deposited by microwave assisted magnetron sputtering. Opto-Electron. Rev. 21, (2013) 233–238.

[13] Zhang, X., Fukushima, A., Jin, M., Emeline, A., Murakami, T., Double-layered TiO_2-SiO_2 nanostructured films with self-cleaning and antireflective properties. J. Phys. Chem. B 110, (2006) 25142–25148.
[14] Vincent, A., Babu, S., Brinley, E., Karakoti, A., Deshpande, S., & Seal, S. Role of Catalyst on Refractive Index Tunability of Porous Silica Antireflective Coatings by Sol−Gel Technique. The Journal of Physical Chemistry C, 111(23), (2007) 8291–8298.
https://doi.org/10.1021/jp0700736
[15] Parkin, I. P., & Palgrave, R. G., Self-cleaning coatings. Journal of Materials Chemistry, 15(17), (2005) 1689. https://doi.org/10.1039/b412803f
[16] Ali, K., Khan, S., MatJafri, M., Effect of double layer (SiO_2/TiO_2) anti-reflective coating on silicon solar cells. Int. J. Electrochem. Sci. 9, (2014) 7865–7874.
[17] B. Gallas, a) A. Brunet-Bruneau, S. Fisson, G. Vuye, and J. Rivory, SiO_2–TiO_2 interfaces studied by llipsometry and x-ray photoemission spectroscopy, Journal Of Applied Physics, 92, 4, (2022) 1922; http://dx.doi.org/10.1063/1.1494843
[18] A. A. Galuska, J. C. Uht, P. M. Adams, and J. M. Coggi, Ion mixing of Ti and TiO y films on SiO_x, Journal of Vacuum Science & Technology A 6, (1988) 2403; https://doi.org/ 10.1116/1.575563.
[19] J. R. Bird, J. S. Williams, Ion Beams for Materials Analysis, Academic Press, Australia, 1989.
[20] I.P. Jain, Garima Agarwal, Ion beam induced surface and interface engineering, Surface Science Reports 66 (2011) 77–172. https://doi.org/10.1016/j.surfrep.2010.11.001